

Video Article

# Tachycardia-Induced Cardiomyopathy As a Chronic Heart Failure Model in Swine

Pavel Hála<sup>1,2</sup>, Mikuláš Miček<sup>1</sup>, Petr Ošťádal<sup>1,2</sup>, David Janák<sup>1,3</sup>, Michaela Popková<sup>1</sup>, Tomáš Bouček<sup>1</sup>, Stanislav Lacko<sup>1</sup>, Jaroslav Kudlička<sup>1</sup>, Petr Neužil<sup>1,2</sup>, Otomar Kittnar<sup>1</sup>

<sup>1</sup>Department of Physiology, First Faculty of Medicine, Charles University

<sup>2</sup>Department of Cardiology, Na Homolce Hospital

<sup>3</sup>Department of Cardiovascular Surgery, Second Faculty of Medicine, Charles University

Correspondence to: Pavel Hála at [pavel.hala@gmx.com](mailto:pavel.hala@gmx.com)

URL: <https://www.jove.com/video/57030>

DOI: [doi:10.3791/57030](https://doi.org/10.3791/57030)

Keywords: Medicine, Issue 132, Animal model, Chronic heart failure, Cardiomyopathy, Extracorporeal life support, Swine, Tachycardia

Date Published: 2/17/2018

Citation: Hála, P., Miček, M., Ošťádal, P., Janák, D., Popková, M., Bouček, T., Lacko, S., Kudlička, J., Neužil, P., Kittnar, O. Tachycardia-Induced Cardiomyopathy As a Chronic Heart Failure Model in Swine. *J. Vis. Exp.* (132), e57030, doi:10.3791/57030 (2018).

## Abstract

A stable and reliable model of chronic heart failure is required for many experiments to understand hemodynamics or to test effects of new treatment methods. Here, we present such a model by tachycardia-induced cardiomyopathy, which can be produced by rapid cardiac pacing in swine.

A single pacing lead is introduced transvenously into fully anaesthetized healthy swine, to the apex of the right ventricle, and fixated. Its other end is then tunneled dorsally to the paravertebral region. There, it is connected to an in-house modified heart pacemaker unit that is then implanted in a subcutaneous pocket.

After 4 - 8 weeks of rapid ventricular pacing at rates of 200 - 240 beats/min, physical examination revealed signs of severe heart failure - tachypnea, spontaneous sinus tachycardia, and fatigue. Echocardiography and X-ray showed dilation of all heart chambers, effusions, and severe systolic dysfunction. These findings correspond well to decompensated dilated cardiomyopathy and are also preserved after the cessation of pacing.

This model of tachycardia-induced cardiomyopathy can be used for studying the pathophysiology of progressive chronic heart failure, especially hemodynamic changes caused by new treatment modalities like mechanical circulatory supports. This methodology is easy to perform and the results are robust and reproducible.

## Video Link

The video component of this article can be found at <https://www.jove.com/video/57030/>

## Introduction

The variety of new treatment methods for heart failure (HF), especially the growing worldwide use of mechanical circulatory supports and extracorporeal membrane oxygenation (ECMO) in clinical practice, is reflecting in preclinical experimental testing. The main focus has been on hemodynamic changes caused by the examined treatment modalities, namely on systemic blood pressure<sup>1</sup>, myocardial contractility, pressure and volume changes in heart chambers and heart work<sup>2,3</sup>, arterial blood flow in systemic and peripheral arteries, along with metabolic compensation<sup>4</sup> - regional tissue saturation, pulmonary perfusion, and blood gas analysis. Other studies are directed on long-term effects of the circulatory support<sup>5</sup>, concomitant inflammation, or occurrence of hemolysis. All these types of study need a stable biomodel of congestive HF.

Most of the published experiments on left ventricular (LV) performance and hemodynamics of mechanical circulatory support have been performed on experimental models of acute HF<sup>2,6,7,8,9,10</sup>, or even on completely intact hearts. On the other hand, in clinical practice, mechanical circulatory supports are often being applied in a status of circulatory decompensation that develops on the grounds of previously present chronic heart disease. In such situations, the adaptation mechanisms are fully developed and can play important roles in inconsistency of outcomes observed according to the "acuteness or chronicity" of underlying cardiac disease<sup>11</sup>. Therefore, a stable model of chronic HF can offer new insights into pathophysiological mechanisms and hemodynamics. Although there are reasons why the use of chronic HF models is scarce - time consuming preparation, instability of heart rhythm, ethical questions, and mortality rate - their advantages are clear, as they offer presence of long-term neurohumoral activation, general systemic adaptation, functional changes of cardiomyocytes, and structural alterations of heart muscle and valves<sup>12,13</sup>.

In general, the availability and variety of animal models used for hemodynamic studies is wide and offers choice for many specific needs. For these experiments, mostly porcine, canine, ovine, or with smaller settings murine models, are being chosen and offer a good simulation of expected human bodily reactions<sup>14</sup>. Furthermore, forms of single organ experiments are becoming more frequent<sup>15</sup>. To reliably mimic the

pathophysiology of HF, circulation is being artificially deteriorated. Damage to the heart can be caused by various methods, often by either ischemia, arrhythmia, pressure overload, or cardiotoxic effects of drugs, with any of these leading to hemodynamic deterioration of the model. To produce a true model of chronic HF, time has to be provided for developing the long-term adaptation of the whole organism. Such a reliable and stable model is represented well by tachycardia-induced cardiomyopathy (TIC), which can be produced by rapid cardiac pacing in experimental animals.

It has been shown that in predisposed hearts, long-lasting incessant tachyarrhythmias can lead to systolic dysfunction and dilation with decreased cardiac output. The condition referred to as TIC was first described in 1913<sup>16</sup>, widely used in experiments since 1962<sup>17</sup>, and is now a well-recognized disorder. Its origin can lie in various types of arrhythmias - both supraventricular and ventricular tachycardia can lead to progressive deterioration of systolic function, biventricular dilation, and progressive clinical signs of HF including ascites, edemas, lethargy, and ultimately cardiac decompensation leading to terminal HF and, if not treated, death.

Similar effects of circulatory suppression were observed by introduction of high rate cardiac pacing in animal models. In a porcine model, an atrial or ventricular heart rate over 200 beats/minute is potent enough to induce end-stage HF in a period of 3 - 5 weeks (progressive phase) with characteristics of TIC, though interindividual differences do exist<sup>18,19</sup>. These findings correspond well to decompensated cardiomyopathy and are, importantly, preserved also after the cessation of pacing (chronic phase)<sup>19,20,21,22,23</sup>.

Porcine, canine, or ovine TIC models were repeatedly prepared to study the pathophysiology of HF<sup>14</sup>, as changes to the LV mimic the characteristics of dilated cardiomyopathy<sup>24</sup>. The hemodynamic characteristics are well described - increased ventricular end-diastolic pressures, decreased cardiac output, increased systemic vascular resistance, and dilation of both ventricles. In contrast, wall hypertrophy is not observed consistently, and even wall thinning was described by some researchers<sup>25,26</sup>. With progression of ventricular dimensions, regurgitation on atrioventricular valves develops<sup>26</sup>.

In this publication, we present a protocol to produce a TIC by long-term fast cardiac pacing in swine. This biomodel represents potent means to study decompensated dilated cardiomyopathy, hemodynamics of progressive chronic HF with low cardiac output, and effects of applied treatment.

## Protocol

This experimental protocol was reviewed and approved by the Institutional Animal Expert Committee at First Faculty of Medicine, Charles University, and was performed at the University experimental laboratory, Department of Physiology, First Faculty of Medicine, Charles University in Prague, Czech Republic, in accordance with Act No. 246/1992 Coll., on the protection of animals against cruelty. All animals were treated and cared for in accordance with the Guide for the Care and Use of Laboratory Animals, 8th edition, published by National Academies Press, 2011. All procedures were performed according to standard veterinary conventions and at the completion of each study, the animal was sacrificed and a necropsy performed. Due to suitable anatomy, five healthy crossbred female swine (*Sus scrofa domestica*) up to 6 months of age were included in this experiment. Their mean body weight was  $66 \pm 20$  kg at the day of data collection.

## 1. General Anesthesia

1. After 1 day of fasting, initiate anesthesia by intramuscular administration of midazolam (0.3 mg/kg) and ketamine hydrochloride (15 - 20 mg/kg) to the gluteal region.
2. Insert peripheral cannula into the marginal ear vein for intravenous drug applications.
3. Administer intravenous boluses of propofol (2 mg/kg) and morphine (0.1 - 0.2 mg/kg).
4. Provide animals with oxygen via a facial mask and advance orotracheal intubation with a cuffed endotracheal tube with a diameter of 6.5 - 7.5 mm.
5. Continue the total intravenous anesthesia by combination of propofol (6 - 12 mg/kg/h), midazolam (0.1 - 0.2 mg/kg/h), and morphine (0.1 - 0.2 mg/kg/h), adjusting the doses according to individual responses - suppress spontaneous breaths, corneal reflexes, and motoric response. Protect the animal's eyes with ointment to prevent dryness.
6. Operate the mechanical ventilation by a closed-loop automatic device set to adaptive support ventilation to maintain target end-tidal CO<sub>2</sub> of 38 - 42 mmHg and adequate hemoglobin saturation of 95 - 99%. Monitor all vital functions, especially heart rate and body temperature.
7. Attach the animal by securing its legs gently to the operation table in the supine position.
8. Administer wide spectrum antibiotics - 1 g of cefazolin intravenously through the ear vein cannula.

## 2. Ventricular Lead Implantation

1. Locate surgical sites and shave the skin properly using a razor at (1) the jugular region above the sternocleidomastoid muscle and (2) the unilateral paravertebral region on the back side of the animal's neck.
2. Using the ultrasound vascular probe, visualize the external jugular vein and mark its location on the skin. Locate the carotid artery as well to prevent its injury.
3. After the wide skin disinfection using povidone iodine, cover with a sterile surgical drape with the hole over the marked jugular region.
4. Prepare all necessary tools for pacemaker implantation and keep them sterile. It is crucial to maintain a sterile environment throughout the procedure.
5. Cut the skin parallel above the external jugular vein, form a shallow subcutaneous pocket in soft tissue not more than 10 mm deep. Do not expose any large vessels.
6. From the bottom of the preformed pocket, insert a sheath into the external jugular vein, using the standard Seldinger technique. First, insert a soft-tip guidewire through a 12G puncture needle, and then over the guidewire introduce a 7-French plastic tear away introducer sheath with a dilator.

- Under fluoroscopic guidance, introduce a 58 cm pacing lead through this sheath and position its tip to the apex of the right ventricle. Then, remove the sheath and fixate the active tip of the electrode to the myocardium by screwing out its helix.
- Test the pacing parameters - the lead sensed signal from ventricular electrocardiogram and impedance must be stable, the pacing threshold should be below an amplitude of 1 V with 0.4 ms of pulse duration.
- Pull a rubber sleeve on the pacing lead and fix both together to the bottom of the preformed jugular subcutaneous pocket by two non-absorbable suture braided thread stitches. Importantly, enough length of the pacing lead must be inserted, considering the future possible growth of the animal.

### 3. Subcutaneous Lead Tunneling

- Turn the animal over on its side and disinfect the previously shaved skin region lateral to the backbone, then cover with a sterile surgical drape with a hole. Make sure the jugular subcutaneous pocket and the lead remain sterile.
- Cut the skin lateral to the backbone and form a deep, spacious, subcutaneous pocket. Use dull preparation and stop any possible bleeding.
- Take a soft rubber extension tube from a sterile infusion set and cut off both its ends. Using a tunneling tool, preform a direct subcutaneous tunnel connecting the jugular and dorsal subcutaneous pockets with this extension tube.
- Connect the tube's free end to the ventricular lead by pulling it onto its IS-1 connector and draw the lead through the preformed tunnel into the dorsal subcutaneous pocket by pulling the tube dorsally. It may be useful to secure the connection with a silk tie.
- Remove both the tunneling tool and the extension tube, exposing the ventricular lead from the dorsal subcutaneous pocket.

### 4. Pacemaker Implantation

- Set up the implantable dual-chamber heart pacemaker unit with the "Y" connecting part. The "Y" connection allows a convergent connection of both pacemaker outputs to be joined and connected together to the single pacing lead (**Figure 1** and **Figure 2**). This setting will later provide a wide range of pacing frequencies.
- After connecting the pacing lead, fasten all the IS-1 connection screws in the pacemaker header unit and the "Y" lead connection.
- Hide the whole pacing system in the deep dorsal pocket. There must be enough space to comfortably accommodate the pacemaker unit and any redundant lead.
- Check the final pacing parameters. Make sure that cardiac ventricular pacing is possible from both pacemaker outputs.
- Flush with povidone iodine and close both subcutaneous pockets. Use absorbable braided thread to suture fibrous tissue layers and non-absorbable suture for skin adaptation.

### 5. Postoperative Care

- Observe the animal carefully until it regains sufficient consciousness.
- Continue in a wide spectrum intravenous antibiotic regimen until the wounds are healed - cefazolin 1 g every 12 h. Administer analgesics in appropriate dosing, e.g., morphine 0.2 mg/kg every 6 - 12 h for 3 days by subcutaneous injection. If necessary, make dose adjustments to adequately prevent pain.
- Place the animal in a comfortable, calm facility at room temperature. Allow free access to water and suitable alimentation.
- Dress the wounds with sterile scrubs regularly to preserve clean healing.
- To provide rest after the surgical procedure, keep the pacemaker inhibited by native heart rhythm for at least 3 days.
- Remove the non-absorbable skin sutures when fully healed, approximately 10 - 14 days after the procedure.

### 6. Pacing Protocol

- Start the pacing protocol after an adequate resting period. Initially, increase the paced ventricular heart rate to 200 beats/min by setting the dual-chamber pacemaker to mode D00, 100 beats/min, and concomitantly adjusting the AV delay to 300 ms (to exactly match the pace to pace interval, see **Table 1**). Select the unipolar pacing in both outputs.
- Increase stepwise the paced heart rate to 220 beats/min after 1 week and to 240 beats/min after 2 weeks (**Figure 3**). Keep continuous pacing at this frequency unless it is not hemodynamically tolerated. If the HF progresses too quickly, reduce the paced heart rate before increasing it again after another week.
- Use auscultation of heart beat, ECG, and pacemaker interrogation daily to verify the heart rate and constant pacing parameters, including battery life.

### 7. Heart Failure Induction and Monitoring

- Ensure regular care by a specialized veterinarian and monitor the animal's general health status. Clinical observations of increasing native heart and respiratory rates, evaluation of peripheral pulse oximetry, and reduction in spontaneous physical activity or appetite provide information about HF progression.
  - Use the advantage of wireless transcutaneous pacemaker interrogation and, if possible, continuous ECG recording - frequent non-sustained ventricular tachycardias (VT) are a sign of severe HF progression.
  - Use echocardiographic assessments to reveal the structural and functional heart changes. Pay attention to find an optimal image window according to porcine anatomy and heart dilation - for a typical 4 chamber view, place the transducer to the right just below the xiphoid and angle it to point to the neck or left shoulder. For short-axis views, use intercostal windows. Reduction of ventricular ejection fraction in native heart rhythm and atrioventricular regurgitations should be noticeable after a few weeks.
- NOTE: Significant interindividual differences of high rate ventricular pacing tolerance exist. Therefore, frequent monitoring and individually adapted adjustment of the pacing protocol are necessary.

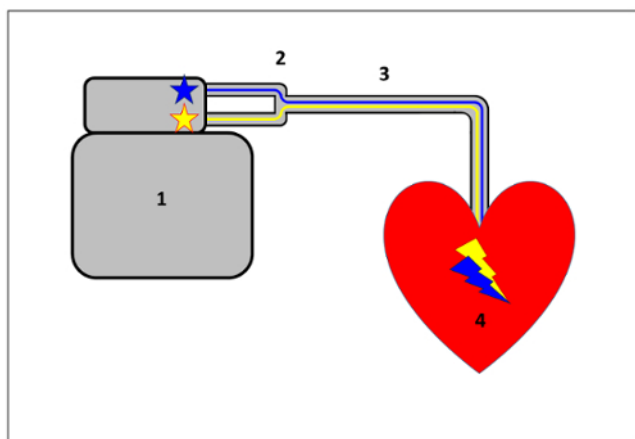


**Figure 1: Heart pacing unit schematic.** The dual-chamber pacemaker (1), a "Y" shaped adapter (2) conducting convergently both pacemaker outputs together to a single pacing lead (3). The tip of the lead is fixated into the apical part of the RV cavity (4). This setting provides a wide range of high pacing frequencies. [Please click here to view a larger version of this figure.](#)

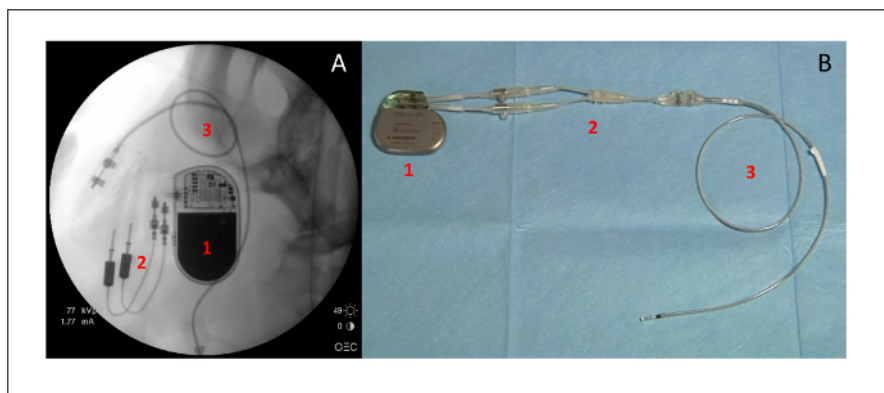


**Figure 2: Heart pacing unit.** X-ray (A) and photography (B) of the dual-chamber pacemaker (1), a "Y" shaped adapter (2), and the ventricular pacing lead (3). [Please click here to view a larger version of this figure.](#)

Desired HR	Set pacemaker rate	Pace to pace interval
beats/min	beats/min	ms
200	100	300
220	110	270
240	120	250
250	125	240

**Table 1: Pacemaker parameters.** To allow high rate cardiac pacing with the implanted in-house-modified dual-chamber pacemaker unit, the table shows the desired paced heart rate (HR) and matching pace to pace interval values. The pacemaker must be set to D00 operation mode at a rate of half of the desired HR, and the AV delay set to the corresponding pace to pace interval in milliseconds.



**Figure 3: Pacing protocol.** The progressive phase of the TIC induction starts after a resting period of 3 days. Then, the pacemaker is set to DDD mode with a pacing frequency of 50% of the desired paced frequency, and AV delay is set to the matching pace to pace interval (see Table 1). Thanks to the "Y" shaped adapter, both pacemaker outputs are conducted to a single pacing lead. bpm = beats/minute. [Please click here to view a larger version of this figure.](#)

## Representative Results

**Testing the model:** After signs of decompensated chronic HF became prominent, anesthesia and artificial ventilation were administered again following the principles described above, but dosing was adjusted due to low cardiac output<sup>27</sup>. Due to possible cardiodepressive effects of anesthetics, careful intensive monitoring of vital functions is necessary.

The animal was attached in the supine position and all invasive approaches commenced. The femoral vein and artery and jugular vein were punctured and intravascular approaches ensured by standard percutaneous intraluminal sheaths. Right carotid and subclavian arteries were surgically exposed and circumjacent ultrasound flow probes of appropriate sizes were attached, enabling the obtainment of continuous blood flow measurements<sup>28</sup>.

Central venous pressure (CVP) was measured via the jugular vein using a standard invasive method with a fluid-filled pressure transducer, but a high-sensitivity pressure sensor equipped catheter in the thoracic aorta was used for systemic arterial pressure measurements. Regional tissue oxygenation was monitored by near-infrared spectroscopy with sensors placed on the head and right forearm representing the brain and peripheral tissue oxygen saturation levels (rSO<sub>2</sub>)<sup>29</sup>. A transthoracic echocardiographic probe was used for 2D and color Doppler imaging. Data from ECG, heart rate, pulse oximetry, blood pressures, capnometry, and rectal temperature were centralized on a bed-side monitor for immediate control. A balloon Swan-Ganz catheter was introduced through a femoral vein sheath to the pulmonary artery allowing readings of thermodilution derived continuous cardiac output (CO)<sup>30</sup> and mixed venous hemoglobin saturation (SvO<sub>2</sub>). Through the aortic valve, a pressure-volume (PV) catheter was introduced retrogradely to the LV cavity. This PV conductance catheter enabled the registration of instant volume and pressure in the LV chamber<sup>31,32,33,34</sup>, and its stable position was guided by fluoroscopy and echocardiography to obtain optimal PV loop morphology (**Figure 4** and **Figure 5**). Measured LV parameters included end-diastolic pressure and volume (EDP and EDV), end-systolic volume (ESV), LV peak pressure (LV PP), and maximal positive change of LV pressure, defined as the first time derivative of LV pressure normalized to EDV (dP/dt<sub>max</sub> / EDV), which then represents a preload independent index of LV contractility<sup>35,36</sup>. Additional calculated parameters were stroke volume (SV = EDV - ESV), left ventricular ejection fraction (EF = SV / EDV), and averaged arterial flow in the carotid and subclavian arteries. Fluoroscopic guidance and X-ray imaging were conducted by a C-arm throughout the protocol. After conclusion of the experimental measurements, euthanasia by intravenous potassium overdose and autopsy were performed. The heart was exposed, cut out from the chest, emptied of blood, weighed, and investigated for structural abnormalities.

All data were acquired in native sinus rhythm after the rapid ventricular pacing had been stopped abruptly and time had been provided for stabilization to steady state conditions. Parameters were then recorded and sets of data averaged from three end-expiratory time points. If present, premature beats were omitted from the analyses. All values are expressed as mean ± standard deviation.

**Measured results:** Physical examination revealed severe clinical signs of chronic HF in all animals after 4 - 8 weeks of pacing protocol. Detailed results are summarized in **Table 2**.

Initial mean heart rate of sinus rhythm was 100 ± 38 beats/min, the mean aortic blood pressure reached 47 ± 38 mmHg and CVP 14 ± 4 mmHg. Chest X-rays showed heart shadow dilation, with a cardiothoracic ratio of 0.64 ± 0.04 (**Figure 5A**). This is in concordance with transthoracic echocardiography findings. Dilation of all heart chambers, severe systolic dysfunction of both ventricles, and significant mitral and tricuspid regurgitations were apparent on echocardiography. Mean ejection fraction of the left ventricle was below 30% in all animals, the LV wall was judged non-hypertrophic with a thickness of 7 - 10 mm and dyssynchrony of LV contraction was obvious (**Figure 6**).

Thermodilution measured cardiac output in the resting state was 2.9 ± 0.8 L/min and mixed venous blood saturation 62 ± 18% corresponded with inadequate tissue oxygen delivery in this model. Average arterial blood flow in the carotid artery was 211 ± 144 mL/min and in the subclavian artery was 103 ± 108 mL/min. Similarly, regional tissue saturation recorded transcutaneously on the head was only 57 ± 13%, and it was even lower on the right forearm, at 37 ± 13%.

The pressure volume loop obtained from the PV catheter illustrates the detailed hemodynamic measures and work produced by the mechanical activity of the left ventricle during each cardiac cycle (**Figure 4**). Maximum LV peak pressure was reduced to  $49 \pm 32$  mmHg, but EDP remained low at  $7 \pm 4$  mmHg. The measured volumes of the left ventricular chamber were reflective of its dilation and systolic dysfunction. EDV was increased to  $189 \pm 59$  mL and ESV to  $139 \pm 37$  mL. Averaged SV was  $51 \pm 45$  mL and the mean LV ejection fraction was calculated to be  $25 \pm 16\%$ . In addition, a preload independent index of LV contractility can be represented by a  $dP/dt_{\max} / \text{EDV}$  ratio, which was averaged to  $2.2 \pm 1.7$  mmHg/s/mL.

An autopsy confirmed cardiomegaly (**Figure 7**) with a mean heart weight of  $471 \pm 127$  g, which formed 0.7% of body weight. Dilation of all heart chambers and LV wall thinning were stated, and fluid collections were described in pericardial and peritoneal spaces. No shunt or other cardiac anomaly was found in any of the animals.

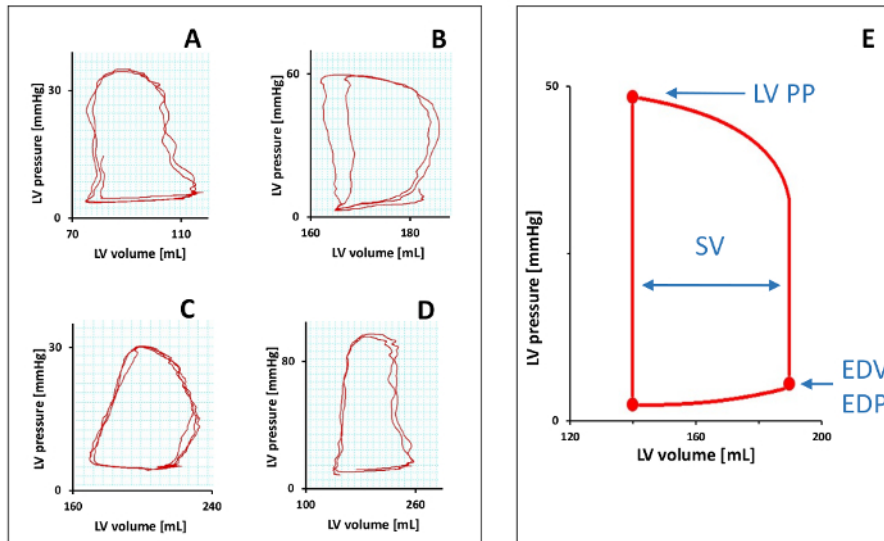


**Figure 4: Pressure-volume measurements.** Samples of direct left ventricular PV loops (**A-D**) and schematic averaged PV loop of all TIC subjects (**E**). LV PP = LV peak pressure, EDP = end-diastolic pressure, EDV = end-diastolic volume, and SV = stroke volume. [Please click here to view a larger version of this figure.](#)

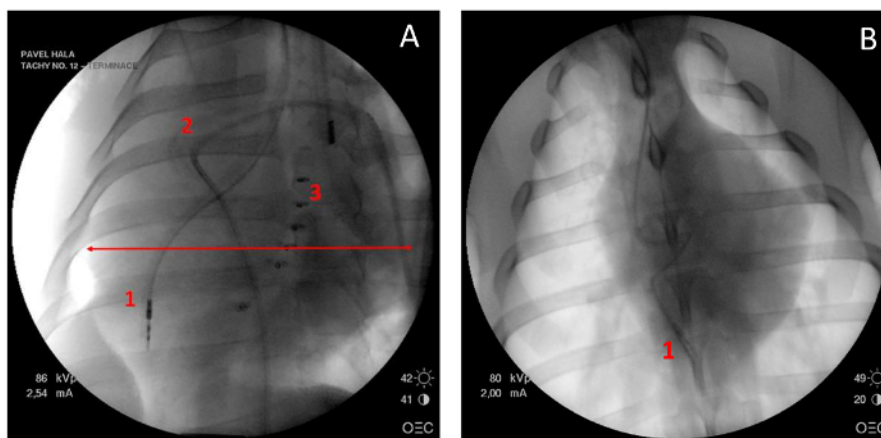


**Figure 5: Chest X-rays.** Enlarged heart shadow (red arrow) and increased cardiothoracic ratio (**A**). Note the pacing lead introduced to the apex of right ventricle (1), Swan-Ganz catheter placed in the pulmonary artery (2), and PV catheter with 5 electrodes in left ventricular chamber (3). For comparison, a chest X-ray of the normal heart from the day of pacemaker implantation (**B**). [Please click here to view a larger version of this figure.](#)



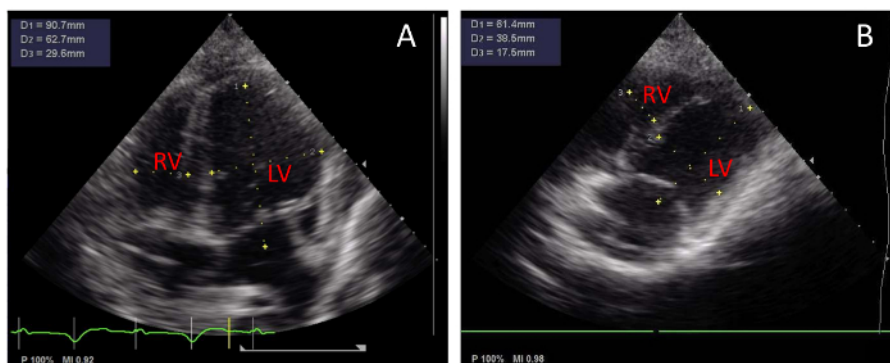


**Figure 6: Transthoracic echocardiography.** Representative tachycardia-induced cardiomyopathy with severe dilation of all heart chambers (**A**) and a similar view obtained before the pacemaker was implanted (**B**), for comparison. Both acquisitions were taken at end-diastole. Notice the visible tip of pacing lead in RV apex in (**A**). RV = right ventricle, and LV = left ventricle. [Please click here to view a larger version of this figure.](#)

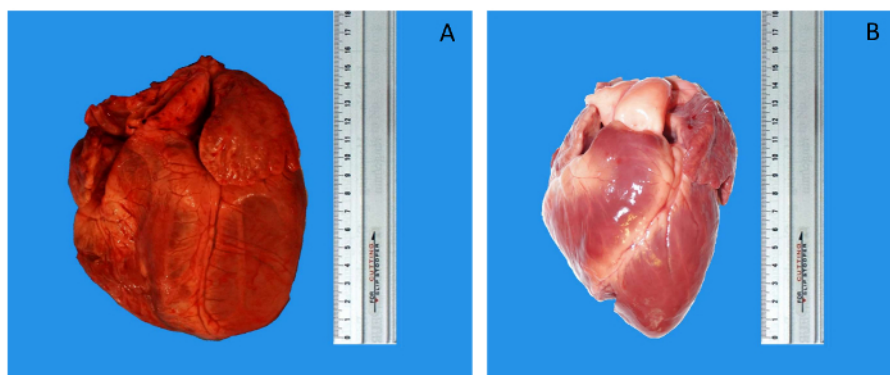


**Figure 7: Photographs of exposed heart.** Cardiomegaly (**A**) after the TIC induction. Normal porcine heart sample for size comparison (**B**) (scales in cm). [Please click here to view a larger version of this figure.](#)

Parameter	TIC value			Units
Imaging				
CTR	0.64	±	0.04	
LV EF		< 30		%
LV EDD	66	±	3	mm
RV EDD	40	±	6	mm
AV regurgitations		severe		
Circulation parameters				
HR	100	±	38	beats/min
MAP	47	±	38	mmHg
CO	2.9	±	0.8	L/min
SvO <sub>2</sub>	62	±	18	%
rSO <sub>2</sub> head	57	±	13	%
rSO <sub>2</sub> right forearm	37	±	13	%
Carotid flow	211	±	144	mL/min
Subclavian flow	103	±	108	mL/min
CVP	14	±	4	mmHg
Pressure-volume acquisition				
LV PP	49	±	32	mmHg
LV EDP	7	±	4	mmHg
LV EDV	189	±	59	mL
LV ESV	139	±	37	mL
SV	51	±	45	mL
LV EF	25	±	16	%
dP/dt <sub>max</sub> / EDV ratio	2.2	±	1.7	mmHg/s/mL
Autopsy				
mean heart weight	471	±	127	g
cardiomegaly, dilation of heart chambers, LV wall thinning, pericardial fluid collections				

**Table 2: Numerical results of the TIC model after cessation of pacing protocol.** All values expressed as mean ± standard deviation. CTR = cardiothoracic ratio, LV EF = LV ejection fraction, LV EDD / RV EDD = LV / RV end-diastolic diameter, AV regurgitations = atrioventricular valve regurgitations, HR = heart rate, MAP = mean aortic pressure, CO = cardiac output, SvO<sub>2</sub> = mixed venous hemoglobin saturation, rSO<sub>2</sub> = regional tissue saturation, CVP = central venous pressure, LV PP = LV peak pressure, LV EDP / LV EDV = LV end-diastolic pressure/volume, LV ESV = LV end-systolic volume, and SV = stroke volume.

## Discussion

Chronic HF is a major health problem that contributes greatly to morbidity and mortality. The pathogenesis and progression of HF in humans is complex, so an appropriate animal model is critical to investigate the underlying mechanisms and to test novel therapeutics that aim to interfere with native severe disease progression. To study its pathogenesis, large animal models are being used for experimental testing.

In general, surgical models of chronic HF closely mimic this disease. When compared to models of acute HF, chronic HF models offer more insight into the pathophysiology, but at the cost of time consuming experimental preparation or higher mortality rate. From the variety of known chronic HF models, we are referring to an appropriate and easily manageable model, represented here by decompensated chronic HF induced by paced tachycardia.

Tachycardia-induced cardiomyopathy as a form of dilated cardiomyopathy is inducible by fast cardiac pacing. The pacing electrode can be located in the ventricles or atria<sup>19,24</sup>. We omitted the supraventricular pacing site to prevent problems possibly caused by atrioventricular block during high pacing frequencies. The ventricular position also improved the stability of the pacing lead fixated in the ventricular apex compared to the atrial position and reduced occurrence of its dislocation. The presented methodology is specifically designed for easy performance, use of widely available equipment, and prevention of complications. Another goal of this method was to easily control chronic HF progression by titration of the pacing protocol.

Bacterial infection complications are a major problem of implants in experimental settings. Generator pocket infections and infective endocarditis are both associated with poor prognoses and would make the experiment futile. Due to porcine anatomy, the jugular region is exposed and if a



pacemaker generator was placed here, healing and preventing contamination would be a difficult task in long-survival experiments. The usage of subcutaneous tunneling enables the location of the pacemaker generator pocket to the dorsal region, which is accessible and can be kept in a hygienic state. The pacemaker is also not within the animal's reach, which considerably improves healing. An alternative approach could be the use of an extracorporeal pacemaker generator attached to the skin surface, but this tactic was shown to be mechanically vulnerable, if long-term animal survival was intended.

All equipment necessary for the described protocol are widely available, and this method is reproducible with basic surgical and catheterization skills. The purpose of the "Y" shaped connection unit is to use a regular dual-chamber pacemaker, as it converges both of its outputs (atrial and ventricular) to the tip of the single pacing lead. These settings allow a wide range of high rate pacing frequencies (200 - 300 beats/min, **Figure 1** and **Table 1**).

The most critical step is the titration of pacing frequencies. Too high from the beginning would cause acute decompensation with no time for the adaptation mechanisms to develop; conversely, titrating the pacing too low would be well tolerated and would prolong the HF induction.

According to previous publications<sup>22,25,37</sup> and the authors' experience, the pacing protocol was defined and started with pacing rate of 200 beats/min, which is above physiological rate of healthy swine in exercise or stress. Subsequently, the frequency was escalated and titrated between 200 and 240 beats/min with respect to individual HF progression<sup>13,19</sup>. Due to interindividual differences in response to fast pacing, the time needed to produce chronic HF with profound signs of decompensation varied from 4 to 8 weeks. An issue here can become the battery life, as such high rate pacing increases energy demands. Especially when the pacing threshold is elevated, regular interrogations are important.

After the pacing protocol, symptoms of chronic HF were prominent consistently in all animals - tachypnea, fatigue, spontaneous tachycardia of >150 beats/min, and systolic murmurs. After further clinical investigation, ascites, pericardial and pleural effusions, non-sustained ventricular tachycardias, dilation of all heart chambers, and significant mitral and tricuspid regurgitations were described. Failing hemodynamics was indicated by arterial hypotension, poor myocardial contractility, low stroke volume, and cardiac output reduced to approximately 50% of a healthy animal's expected normal value<sup>38</sup>. This developed model of tachycardia induced cardiomyopathy matched well to poorly compensated dilated cardiomyopathy and was also preserved after the cessation of pacing<sup>21,39,40</sup>.

The fact that systolic function continues to be severely deteriorated after cessation of pacing makes the model an excellent choice to examine HF in native sinus rhythm. It has been previously shown that tachycardia-induced systolic dysfunction is at least partially reversible in the so-called recovery phase, but the time needed for it to improve or normalize varies significantly between individuals. The pacing protocol duration and aggressiveness of rate titration may be a significant contributor too, as permanent ischemic and fibrotic changes are produced in the myocardium<sup>22,39,40,41</sup>. The persistence of severe systolic dysfunction in the presented model was tested at least for 12 h after the pacing had been ceased<sup>4</sup> and the qualities of the prepared model including neurohumoral dynamics, peripheral vascular abnormalities, and cardiac dysfunction were reflective of human chronic HF<sup>14</sup>.

The presented results demonstrate severely deteriorated hemodynamics, both clinical investigation and measured values indicate induction of HF syndrome. Cardiomegaly was consistently observed by clinical examination, imaging, and autopsy. Heart rate of sinus rhythm after the cessation of fast pacing was elevated from normal resting frequency, but we assume that the influence of cardiodepressive effects of anesthetics could limit this spontaneous tachycardia. Aortic pressures show deep hypotension<sup>42</sup> and CVP was elevated.

Functional reflection is then the failing circulation and tissue hypoperfusion. These are primarily caused by impaired myocardial contraction, as indicated by the low ejection fraction of the left ventricle. Both ventricles were dilated with no extension in wall thickness, and this heart remodeling was grounds for progressive atrioventricular regurgitations and consequently low cardiac output. As no anatomical shunts were found postmortem, the cardiac output was equally low in systemic as well as in pulmonary circulation, and so the thermodilution derived cardiac output measurements in the pulmonary artery were used to calibrate the PV loop volume characteristics.

The brachial and brain regional tissue oxygen saturation as well as the regional blood flow in subclavian and carotid artery suggests centralization of the blood circulation. Their low values show severely reduced tissue perfusion in peripheral as well as in vital organs, which was confirmed by low SvO<sub>2</sub> when compared to the expected normal value of at least 65%<sup>42</sup>. The general low tissue perfusion was in concordance with the measurements of low cardiac output.

Hemodynamics and mechanical work during each cardiac cycle of the left ventricle was well documented by the PV diagram obtained from PV catheter instant measurements. Poor myocardial strength was denoted by maximum LV peak pressure during systole and the dP/dt<sub>max</sub> / EDV ratio, a preload independent index of LV contractility. LV chamber volumes were enlarged during the whole cycle, thus the image of dilated cardiomyopathy. The end-diastolic LV pressure was not increased as high as would be expected in cardiogenic shock. The LV filling pressure remains low, most likely due to high compliance of the LV thin myocardial wall<sup>43</sup>.

In the vast majority of previous TIC studies, porcine and canine models have been used<sup>19</sup>. However, rapid pacing can be used to induce cardiomyopathy in other species, even in small animals. Few studies have demonstrated metabolic effects of acute TIC in rats<sup>44</sup> or myocardial contractility impairment after long-term fast pacing in rabbits<sup>45</sup>.

Although this model is adequately reliable, it has several limitations. Non-sustained ventricular tachycardias are a sign of successful HF induction, but long-lasting VT produce risks of sudden cardiac death. During anesthesia, one of the animals required resuscitation and defibrillation. The wide dispersion of results was partly due to differences in animal body weight. Also, the necessity of anesthesia has to be taken under consideration when reporting the results, especially its influence on heart rate and blood pressure. Blood levels of porcine-specific markers could be useful for assessment of the degree of cardiac remodeling, but the evidence on this front is still lacking. As most of these measurement methods were invasive and thus unrepeatable, we did not provide a baseline or sham subject measurement.

A model of progressive chronic heart failure can be produced by the presented methodology. This technique is easy to perform with widely available equipment, and the results are robust and reproducible. This tachycardia-induced cardiomyopathy offers a valuable object for further experimental studies on hemodynamics, investigation of disease mechanisms and effects of applied treatments.

positives	negatives
chronic heart failure syndrome with systemic adaptation	time consuming model preparation
easy control of disease progression	close monitoring necessary
lead tunneling prevents infective complications	risk of lead dislocation
done with basic surgical and cathetrization skills	risk of malignant arrhythmia
potentially transferable to different animal species	

**Table 3: Overview summarizing the positives and negatives of the presented methodology for tachycardia-induced cardiomyopathy in swine as a model of chronic heart failure.**

## Disclosures

The authors have nothing to disclose.

## Acknowledgements

This work was supported by Charles University research grants GA UK No. 538216 and GA UK No. 1114213.

## References

- Ostadal, P. *et al.* Direct comparison of percutaneous circulatory support systems in specific hemodynamic conditions in a porcine model. *Circ Arrhythm Electrophysiol.* **5** (6), 1202-1206 (2012).
- Ostadal, P. *et al.* Increasing venoarterial extracorporeal membrane oxygenation flow negatively affects left ventricular performance in a porcine model of cardiogenic shock. *J Transl Med.* **13** 266 (2015).
- Shen, I. *et al.* Left ventricular dysfunction during extracorporeal membrane oxygenation in a hypoxemic swine model. *Ann Thorac Surg.* **71** (3), 868-871 (2001).
- Hala, P. *et al.* Regional tissue oximetry reflects changes in arterial flow in porcine chronic heart failure treated with venoarterial extracorporeal membrane oxygenation. *Physiol Res.* **65** (Supplementum 5), S621-S631 (2016).
- Church, J. T. *et al.* Normothermic Ex-Vivo Heart Perfusion: Effects of Live Animal Blood and Plasma Cross-Circulation. *ASAIO J.* (2017).
- Bavaria, J. E. *et al.* Changes in left ventricular systolic wall stress during biventricular circulatory assistance. *Ann Thorac Surg.* **45** (5), 526-532 (1988).
- Shen, I. *et al.* Effect of extracorporeal membrane oxygenation on left ventricular function of swine. *Ann Thorac Surg.* **71** (3), 862-867 (2001).
- Ostadal, P. *et al.* Novel porcine model of acute severe cardiogenic shock developed by upper-body hypoxia. *Physiol Res.* **65** (4), 711-715 (2016).
- Ostadal, P. *et al.* Noninvasive assessment of hemodynamic variables using near-infrared spectroscopy in patients experiencing cardiogenic shock and individuals undergoing venoarterial extracorporeal membrane oxygenation. *J Crit Care.* **29** (4), 690 e611-695 (2014).
- Mlcek, M. *et al.* Hemodynamic and metabolic parameters during prolonged cardiac arrest and reperfusion by extracorporeal circulation. *Physiol Res.* **61** (Suppl 2) S57-65 (2012).
- Tarzia, V. *et al.* Extracorporeal life support in cardiogenic shock: Impact of acute versus chronic etiology on outcome. *J Thorac Cardiovasc Surg.* **150** (2), 333-340 (2015).
- Howard, R. J., Stopps, T. P., Moe, G. W., Gotlieb, A., Armstrong, P. W. Recovery from heart failure: structural and functional analysis in a canine model. *Can J Physiol Pharmacol.* **66** (12), 1505-1512 (1988).
- Moe, G. W., Armstrong, P. Pacing-induced heart failure: a model to study the mechanism of disease progression and novel therapy in heart failure. *Cardiovasc Res.* **42** (3), 591-599 (1999).
- Power, J. M., Tonkin, A. M. Large animal models of heart failure. *Aust N Z J Med.* **29** (3), 395-402 (1999).
- Trahanas, J. M. *et al.* Achieving 12 Hour Normothermic Ex Situ Heart Perfusion: An Experience of 40 Porcine Hearts. *ASAIO J.* **62** (4), 470-476 (2016).
- Gossage, A. M., Braxton Hicks, J. A. On auricular fibrillation. *Quarterly Journal of Medicine.* **6** 435-440 (1913).
- Whipple, G. H., Sheffield, L. T., Woodman, E. G., Theophilis, C., Friedman, S. Reversible congestive heart failure due to chronic rapid stimulation of the normal heart. *Proceedings of the New England Cardiovascular Society.* **20** (1), 39-40 (1962).
- Spinale, F. G., Grine, R. C., Tempel, G. E., Crawford, F. A., Zile, M. R. Alterations in the myocardial capillary vasculature accompany tachycardia-induced cardiomyopathy. *Basic Res Cardiol.* **87** (1), 65-79 (1992).
- Shinbane, J. S. *et al.* Tachycardia-induced cardiomyopathy: a review of animal models and clinical studies. *J Am Coll Cardiol.* **29** (4), 709-715 (1997).
- Moe, G. W., Stopps, T. P., Howard, R. J., Armstrong, P. W. Early recovery from heart failure: insights into the pathogenesis of experimental chronic pacing-induced heart failure. *J Lab Clin Med.* **112** (4), 426-432 (1988).
- Takagaki, M. *et al.* Induction and maintenance of an experimental model of severe cardiomyopathy with a novel protocol of rapid ventricular pacing. *J Thorac Cardiovasc Surg.* **123** (3), 544-549 (2002).
- Tomita, M., Spinale, F. G., Crawford, F. A., Zile, M. R. Changes in left ventricular volume, mass, and function during the development and regression of supraventricular tachycardia-induced cardiomyopathy. Disparity between recovery of systolic versus diastolic function. *Circulation.* **83** (2), 635-644 (1991).
- Schmitto, J. D. *et al.* Large animal models of chronic heart failure (CHF). *J Surg Res.* **166** (1), 131-137 (2011).
- Spinale, F. G. *et al.* Chronic supraventricular tachycardia causes ventricular dysfunction and subendocardial injury in swine. *Am J Physiol.* **259** (1 Pt 2), H218-229 (1990).

25. Chow, E., Woodard, J. C., Farrar, D. J. Rapid ventricular pacing in pigs: an experimental model of congestive heart failure. *Am J Physiol.* **258** (5 Pt 2), H1603-1605 (1990).
26. Howard, R. J., Moe, G. W., Armstrong, P. W. Sequential echocardiographic-Doppler assessment of left ventricular remodelling and mitral regurgitation during evolving experimental heart failure. *Cardiovasc Res.* **25** (6), 468-474 (1991).
27. Roberts, F., Freshwater-Turner, D. Pharmacokinetics and anaesthesia. *Contin Educ Anaesth Crit Care Pain* **7** (1): 25-29. (2007).
28. Carter, B. S., Farrell, C., Owen, C. Microsurgical clip obliteration of middle cerebral aneurysm using intraoperative flow assessment. *J Vis Exp.* (31) (2009).
29. Wolf, M., Ferrari, M., Quaresima, V. Progress of near-infrared spectroscopy and topography for brain and muscle clinical applications. *J Biomed Opt.* **12** (6), 062104 (2007).
30. Mateu Campos, M. L. *et al.* [Techniques available for hemodynamic monitoring. Advantages and limitations]. *Med Intensiva.* **36** (6), 434-444 (2012).
31. Baan, J. *et al.* Continuous measurement of left ventricular volume in animals and humans by conductance catheter. *Circulation.* **70** (5), 812-823 (1984).
32. Ellenbroek, G. H. *et al.* Primary Outcome Assessment in a Pig Model of Acute Myocardial Infarction. *J Vis Exp.* (116) (2016).
33. Townsend, D. Measuring Pressure Volume Loops in the Mouse. *J Vis Exp.* (111) (2016).
34. van Hout, G. P. *et al.* Admittance-based pressure-volume loops versus gold standard cardiac magnetic resonance imaging in a porcine model of myocardial infarction. *Physiol Rep.* **2** (4), e00287 (2014).
35. Kass, D. A. *et al.* Comparative influence of load versus inotropic states on indexes of ventricular contractility: experimental and theoretical analysis based on pressure-volume relationships. *Circulation.* **76** (6), 1422-1436 (1987).
36. Glower, D. D. *et al.* Linearity of the Frank-Starling relationship in the intact heart: the concept of preload recruitable stroke work. *Circulation.* **71** (5), 994-1009 (1985).
37. Hendrick, D. A., Smith, A. C., Kratz, J. M., Crawford, F. A., Spinale, F. G. The pig as a model of tachycardia and dilated cardiomyopathy. *Lab Anim Sci.* **40** (5), 495-501 (1990).
38. Wyler, F. *et al.* [The Gottinger minipig as a laboratory animal. 5. Communication: cardiac output, its regional distribution and organ blood flow (author's transl)]. *Res Exp Med (Berl).* **175** (1), 31-36 (1979).
39. Cruz, F. E. *et al.* Reversibility of tachycardia-induced cardiomyopathy after cure of incessant supraventricular tachycardia. *J Am Coll Cardiol.* **16** (3), 739-744 (1990).
40. Umana, E., Solares, C. A., Alpert, M. A. Tachycardia-induced cardiomyopathy. *Am J Med.* **114** (1), 51-55 (2003).
41. Dixon, J. A., Spinale, F. G. Large animal models of heart failure: a critical link in the translation of basic science to clinical practice. *Circ Heart Fail.* **2** (3), 262-271 (2009).
42. Xanthos, T. *et al.* Baseline hemodynamics in anesthetized landrace-large white swine: reference values for research in cardiac arrest and cardiopulmonary resuscitation models. *J Am Assoc Lab Anim Sci.* **46** (5), 21-25 (2007).
43. Little, W. C. Diastolic dysfunction beyond distensibility: adverse effects of ventricular dilatation. *Circulation.* **112** (19), 2888-2890 (2005).
44. Montgomery, C., Hamilton, N., Ianuzzo, C. D. Effects of different rates of cardiac pacing on rat myocardial energy status. *Mol Cell Biochem.* **102** (2), 95-100 (1991).
45. Qin, F., Shite, J., Mao, W., Liang, C. S. Selegiline attenuates cardiac oxidative stress and apoptosis in heart failure: association with improvement of cardiac function. *Eur J Pharmacol.* **461** (2-3), 149-158 (2003).